

Research Article

Mathematical Model for Spread and Control of Cocoa Black Pod Disease

Adebayo Adeniran^{*} , Adeniyi Onanaye, Olawale Adeleke

Department of Mathematics and Statistics, Redeemer's University, Ede, Nigeria
E-mail: adeniran9867@run.edu.ng

Received: 20 May 2023; **Revised:** 26 July 2023; **Accepted:** 14 August 2023

Abstract: Black pod disease is a major threat to cocoa production worldwide. A mathematical model for the spread of cacao black pod disease is presented in this article. The model takes into account several variables that influence the spread of the disease. A set of differential equations that are numerically solved using Runge-Kutta method embedded in MATLAB software are used to simulate the dynamics of disease transmission which form the basis of the model. Utilizing information from the literature and ecological observations from cocoa fields in West Africa, where black pod disease poses a serious threat to the production of cocoa, the model was verified. The model's outcomes highlight the significance of early detection and rapid intervention in mitigating the severity of cocoa black pod disease outbreaks. Moreover, it emphasizes the importance of adopting integrated disease management approaches that consider fungicide administration and removal of infected pods. The usefulness of mathematical modeling as a tool for understanding and managing cocoa black pod disease is illustrated by this study.

Keywords: cocoa, differential equations, basic reproductive number, disease-free equilibrium, endemic equilibrium, asymptotic stability

MSC: 92xx, 91-10

1. Introduction

The Millennium Development Goals (MDGs) were a set of global development goals set by the United Nations (UN) in the year 2000, which were meant to address important problems like poverty, hunger, health, education, gender equality, environmental sustainability, and global partnership [1].

Cocoa production is a very important part of many emerging countries' economy, especially in Africa, Central America, and Southeast Asia. It has a close connection to the MDGs and is a very important part of that sector [2].

Cocoa Black Pod Disease (CBPD) is one of the most devastating diseases affecting cocoa production worldwide, causing major yield losses and economic devastation to farmers and the cocoa industry, hence impeding the MDGs for hunger and poverty alleviation [3]. The disease is caused by several species of *Phytophthora* (P), including *P. megakarya*, *P. palmivora*, *P. capsici*, and *P. tropicalis* [4]. The fungal disease poses a serious danger to the production of cocoa and the livelihoods of farmers in many places since it can result in yield losses of up to 90% in affected areas. Dark lesions on the pods, which can spread quickly and cause the pods to rot and fall from the tree, are signs of cocoa

black pod disease. Infection by the fungus on leaves, pods, stems, and shoots can result in defoliation and dieback [5-6].

The destructive cocoa pathogen *P. megakarya* can spread both directly and indirectly to the cocoa tree and pods. While indirect transmission involves vectors that spread the infection from one plant to another, direct transmission entails the pathogen coming into direct contact with the plant. Direct means of transmission of *P. megakarya* in cocoa include: Rainfall: Rainfall can directly disperse *P. megakarya* spores from infected plant tissues to healthy tissues, particularly during the rainy season when the spores are more abundant and favorable environmental conditions exist [7]. Infected plant debris: The pathogen can survive in infected plant debris and can directly infect healthy plants that come into contact with the debris [5, 7]. Soil-borne transmission: The pathogen can survive in the soil for several years and can directly infect cocoa roots through the soil [7]. Indirect means of transmission of *P. megakarya* in cocoa include: Insects: Several insects have been found to be vectors of *P. megakarya*, including the cocoa pod borer (*Conopomorpha cramerella*) and several species of beetles and flies [8], these insects can indirectly transmit the pathogen to healthy plants as they feed on the tissues of infected plants. Human activity: Human activities such as pruning and harvesting can indirectly transmit the pathogen to healthy plants as workers move from infected to healthy plants [7].

Cocoa trees produce small, delicate flowers that grow directly from the trunk and branches. The flowers are usually white or pale pink in color. Pollination occurs during this stage, either through self-pollination or with the help of pollinators like insects, once pollinated, the flowers begin to develop into cocoa pods, this stage is usually referred to as Cherelles stage. After successful pollination, the cocoa pods start to grow from the base of the flowers, initially, they are small, green, and hard. At this stage, the cocoa beans are tiny and undeveloped, and the pods enlarge and become more prominent, at this point, the pods start to change color, transitioning from green to yellow, red, or purple, depending on the cocoa variety. The color change indicates that the cocoa pods are approaching maturity (usually this stage is referred to as the young and mature pod stage). The maturity stage is the ideal time for cocoa pod harvesting. During this phase, the pods have reached their full size and have fully changed color (ripe) and ready for harvesting [7-8]. Mathematical modeling is a useful technique in plant disease management for determining disease transmission and developing control measures. Most epidemic models reported in the literature were created using the groundbreaking research of Kermack and McKendrick [9]. Plant-Disease Mathematical Models (Deterministic and stochastic models) can be used to broadly categorize mathematical models of plant diseases. Deterministic models are founded on equations that describe the spread of disease under specific conditions [10], whereas stochastic models account for random factors that influence the spread of disease [11]. Both types of models have been applied to the study of the spread of plant diseases, and their utility depends on the disease's specific characteristics and the available data [10-11]. The susceptible-infectious-recovered (SIR) model is a widely applied deterministic model, this paradigm classifies the population into three distinct subgroups: susceptible, infectious, and recovered.

Understanding the transmission dynamics of CBPD and developing effective control strategies requires the use of mathematical modeling. Several mathematical models have been developed in recent years to characterize the spread of plant diseases and evaluate the effectiveness of various control approaches [12-14]. There are only a few studies in the literature on the mathematical modeling of cocoa disease [8, 15]. To control the spread of the disease, the study intends to develop, assess, and apply a new model that captures the control and dynamics of the disease coupled with direct and indirect modes of transmission.

The possibility of a parasitic infection on cacao pods causes cocoa growers and researchers great concern, but the underlying causes of the spread of *P. megakarya* on cacao remain unclear. As a result, there is a growing need for a fundamental understanding of the *P. megakarya* epidemiology in order to develop workable management strategies; Nembot et al.'s [8] work has made a significant contribution in this regard, particularly in the area of transmission. In this work, we included Latent compartment (L), Removed compartment (R) and Treatment compartment (T) to better the model of Nembot et al. [8] in order to treat the disease in the most effective way. The most important parameters in determining the severity of the condition were also identified using sensitivity analysis of parameters.

The motivation behind this research lies in the critical importance of cocoa as a major cash crop for numerous cocoa-producing regions, serving as a significant source of income and livelihood for millions of farmers. However, the persistent and unpredictable nature of cocoa black pod disease outbreaks severely impacts cocoa yields, leading to substantial economic losses and compromising food security.

The article introduces a groundbreaking contribution to the field of cocoa black pod disease research. Through its comprehensive integration of epidemiological and ecological factors, predictive capabilities, evaluation of diverse

control strategies, sensitivity analysis, and implications for sustainable cocoa production, our study offers a novel and robust foundation for combating this devastating pathogen and safeguarding the global cocoa industry.

This paper is arranged as follows: Section 2 describe the model formulation of the study. In section 3, analysis of the model was considered. Sensitivity analysis was described in section 4, Numerical simulation, Finding of study, Discussion and Conclusion were discussed in section 5, 6 and 7 respectively.

2. Model formulation

In this section, we present a mathematical model that describes infection transmission among the infectious environment, infected pods, and healthy cocoa pods. The total population $N(t)$ at time $t > 0$ was subdivided according to stages of cocoa pod development. The first stage of cocoa pod development, the floral and formation of pod state, is called Cherelles ($S_c(t)$), followed by the young and mature pod stage ($S_p(t)$), and finally the ripe pod stage ($S_r(t)$). $L(t)$ represents the latency compartment when a microbe's persistence in a host causes host harm without disrupting homeostasis sufficiently to trigger clinical signs or disease. The infectious pod compartment is represented by $I(t)$. $I_s(t)$ denotes the secondary infection(indirect transmission), likewise the primary infection(direct transmission) $I_p(t)$ are infection transmitted through the spores of infected pods to healthy pods. $T(t)$ denotes the treated pods compartment and $R(t)$ represent the removed pod compartment.

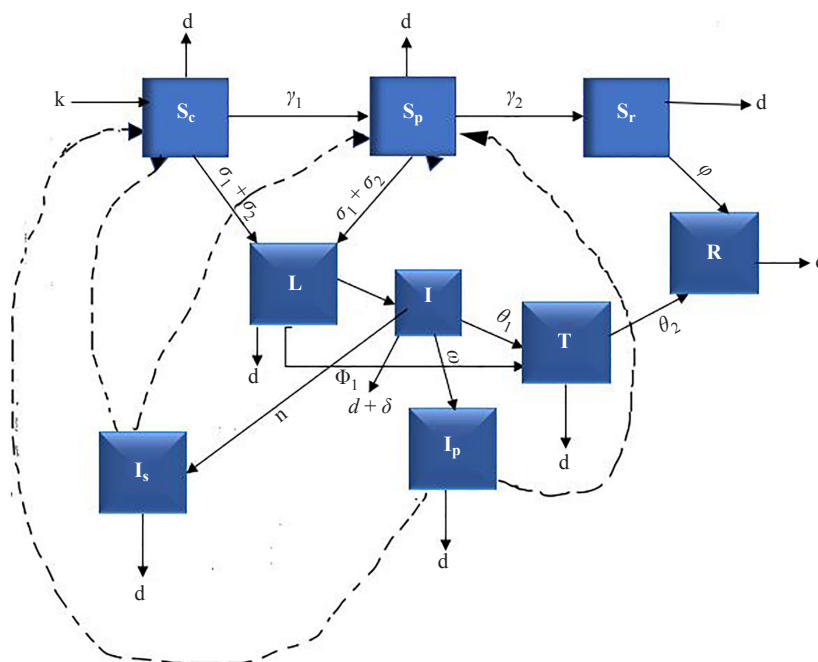


Figure 1. Compartmental diagram for the transmission dynamics of CBPD

The model diagram as shown in Figure 1 describe the diagrammatically representation of the transmission of the disease with respect to the of stages of pod development, differential equation was used to transform the model information to a system of differential equation where the inflow of new susceptible into the Cherelles compartment was considered at rate k (recruitment rate), this compartment reduces by γ_1 which is the rate of transmission from Cherelles to young and mature stage, d the natural death rate at Cherelles stage and the forces of infection rate (σ_1 & σ_2) denoted by

$$\sigma_1 = \frac{\beta_1 I_s}{P + I_s}, \text{ see [8] for details} \quad (1)$$

$$\sigma_2 = \frac{\beta_2 I_p}{P + I_p}, \text{ see [8] for more details} \quad (2)$$

where P is the Michaelis constant for the disease transmission of pod infection, β_1 & β_2 denotes the primary and secondary infection rate at Cherelles stage respectively.

The young and mature susceptible compartment increases through transmission rate from Cherelles compartment γ_1 and reduces due to ripening rate γ_2 the ripening rate of young and mature pods, d the natural death rate at young and mature pod stage and forces of infection σ_3 & σ_4 , which is denoted by

$$\sigma_3 = \frac{\beta_3 I_s}{P + I_s}, \text{ see [8] for more details} \quad (3)$$

$$\sigma_4 = \frac{\beta_4 I_p}{P + I_p}, \text{ see [8] for more details} \quad (4)$$

where β_3 & β_4 denotes the primary and secondary infection rate at mature pod stage respectively.

The ripening susceptible compartment increases by γ_2 the ripening rate of young and mature pods and decreases by d the natural death rate at this stage and ψ , which is the pod harvesting rate.

The latent compartment increases by $\sigma_1, \sigma_2, \sigma_3, \sigma_4$ and decreases by d , the natural pod death rate, α , the rate of transmission from latent to infectious state, ϕ_1 , rate at which pod is treated with fungicide.

Infectious compartment increases due to α and reduces through the releasing rate of spores η, ω & θ_1 , natural death d , rate of infected pod removal δ .

The treated pods compartment increases due to the effective rate of fungicide spraying θ_1 and reduces due to the infected pod recovery rate θ_2 and natural death d .

The recovery compartment increases due to the inflow θ_2 from Treatment compartment, ripe infected pod γ_3 from infected class, healthy ripe pod harvested rate ψ and the compartment reduces due to the natural death d .

The production rate of spore release rate n causes the secondary infection compartment to grow, and the natural death rate d causes it to reduce. The main infection compartment rises as a result of the spore release rate ω and reduces as a result of the natural death rate d .

The set of first-order ordinary differential equations that are nonlinear governing the transmission in the Figure 1 is provided as follows, under the aforementioned assumptions:

$$\frac{dS_c}{dt} = k - (d + \sigma_1 + \sigma_2 + \gamma_1)S_c$$

$$\frac{dS_p}{dt} = \gamma_1 S_c - (\sigma_3 + \sigma_4 + \gamma_2 + d)S_p$$

$$\frac{dS_r}{dt} = \gamma_2 S_p - (d + \psi)S_r$$

$$\begin{aligned} \frac{dL}{dt} &= (\sigma_1 + \sigma_2)S_c + (\sigma_3 + \sigma_4)S_p - (\alpha + d)L \\ \frac{dI}{dt} &= \alpha L - (n + \omega + \theta_1 + d + \delta)I \\ \frac{dT}{dt} &= \theta_1 I - (\theta_2 + d)T \\ \frac{dR}{dt} &= \psi S_r + \theta_2 T - dR \\ \frac{dI_s}{dt} &= nI - dI_s \\ \frac{dI_p}{dt} &= \omega I - dI_p \end{aligned} \tag{5}$$

subject to the initial conditions

$$(S_c(0), S_p(0), S_r(0), L(0), I(0), T(0), R(0), I_s(0), I_p(0)) \geq 0. \tag{6}$$

3. Model analysis

In this section, we considered the analysis of the model by considering its feasibility, positivity, disease free and endemic equilibrium.

3.1 Boundedness (feasibility) of the model

Theorem 3.1 The domain $\Omega = \{(S_c, S_p, S_r, L, I, T, R, I_s, I_p) \in \mathfrak{R}_+^9; 0 \leq N(t) \leq \frac{k}{d}\}$ for the model system (5) with non negative starting conditions in \mathfrak{R}_+^9 , is positively invariant and attracting.

Proof. Let

$$N(t) = S_c(t) + S_p(t) + S_r(t) + L(t) + I(t) + T(t) + R(t) + I_s(t) + I_p(t). \tag{7}$$

Then, we have

$$\frac{dN(t)}{dt} = \frac{dS_c(t)}{dt} + \frac{dS_p(t)}{dt} + \frac{dS_r(t)}{dt} + \frac{dL(t)}{dt} + \frac{dI(t)}{dt} + \frac{dT(t)}{dt} + \frac{dR(t)}{dt} + \frac{dI_s(t)}{dt} + \frac{dI_p(t)}{dt} \tag{8}$$

$$\frac{dN}{dt} = k - dN(t) - \delta I(t) \tag{9}$$

(9) is known as model population dynamics (see [16] for more details). In the absence of infection $\delta = 0$, (9) is reduced

to a differential inequality,

$$\frac{dN}{dt} \leq k - dN(t) \tag{10}$$

on integrating the differential inequality (10), we have

$$-\frac{1}{d} \ln(k - dN(t)) \leq t + C_o, \tag{11}$$

where C_o is constant of integration

$$k - dN(t) \leq Ae^{-dt}, \tag{12}$$

where A is a constant, $A = e^{-d_o C_o}$.

At $t = 0$,

$$k - dN(0) \leq A \tag{13}$$

substituting equation (13) into (12) yields

$$N(t) \leq \frac{k}{d}(1 - e^{-dt}) + N(0)e^{-dt},$$

as $t \rightarrow \infty$

$$N(t) \leq \frac{k}{d}, \tag{14}$$

hence, the feasible (boundedness) solution for the system (5) is given by

$$\Omega = \left\{ (S_c, S_p, S_r, L, I, T, R, I_s, I_p) \in \mathfrak{R}_+^9; 0 \leq N(t) \leq \frac{k}{d} \right\}$$

is a compact forward invariant set. Every solution with a starting condition of \mathfrak{R}_+^9 thus stays in the Ω region for $t > 0$. Thus, the model system (5) is well-posed from a mathematical and epidemiological perspective. \square

3.2 Positivity of solutions

The following theorem will prove that all solutions of the system (5) with positive initial data will continue to be positive for all time $t > 0$, although it has to be verified.

Theorem 3.2 System (5) maintains the positivity of the solutions, which means that the system's initial conditions for the state variables are always greater than zero for all time t .

Proof. Considering the first equation in system (5),

$$\frac{dS_c}{dt} = k - (d + \sigma_1 + \sigma_2 + \gamma_1)S_c$$

$$\frac{dS_c}{dt} \geq -(d + \sigma_1 + \sigma_2 + \gamma_1)S_c \quad (15)$$

Integrating the inequality in (15) gives

$$S_c(t) \geq B e^{-(d + \sigma_1 + \sigma_2 + \gamma_1)t}, \quad (16)$$

where C_1 is constant of integration and $B = e^{C_1}$ at $t = 0$, equation (16) becomes

$$S_c(0) \geq B \quad (17)$$

inserting (17) into (16) gives

$$S_c(t) \geq S_c(0)e^{-(d + \sigma_1 + \sigma_2 + \gamma_1)t} \geq 0 \quad (18)$$

since

$$(d + \sigma_1 + \sigma_2 + \gamma_1)t > 0, \quad (19)$$

hence $S_c(t)$ is positive for $t > 0$. Similar proof can be established for the positivity of other solutions in equation (5). Thus, the solution of the model in (5) are positive for all time $t > 0$. \square

3.3 Disease Free Equilibrium (DFE)

When there are no infections among the pods population, it is said to be in a condition of DFE, all classes will be denoted by (o) . In the absence of disease, we assume that $L^o = I^o = I_p^o = I_s^o$, (see [17-19] for details).

Let

$$E^o = (S_c^o, S_p^o, S_r^o, L^o, I^o, T^o, R^o, I_s^o, I_p^o) \quad (20)$$

be the DFE state for the Pod population, therefore the DFE point is given by

$$S_c^o = \frac{k}{d + \gamma_1}$$

$$S_p^o = \frac{\gamma_1 k}{(d + \gamma_1)(d + \gamma_2)}$$

$$S_r^o = \frac{\gamma_2 \gamma_1 k}{(d + \gamma_1)(d + \gamma_2)(d + \psi)}$$

$$R^o = \frac{\psi\gamma_2\gamma_1k}{d(d+\gamma_1)(d+\gamma_2)(d+\psi)} \quad (21)$$

hence, the DFE of the model (5) is

$$E^o = \left(\frac{k}{d+\gamma_1}, \frac{\gamma_1k}{(d+\gamma_1)(d+\gamma_2)}, \frac{\gamma_2\gamma_1k}{(d+\gamma_1)(d+\gamma_2)(d+\psi)}, 0, 0, 0, \frac{\psi\gamma_2\gamma_1k}{d(d+\gamma_1)(d+\gamma_2)(d+\psi)}, 0, 0 \right)$$

3.4 Endemic Equilibrium State (EES)

EES (E^+) is the state where the disease persist in the pod population (see [18, 20-21] for details on how to determine EES). Let

$$E^+ = (S_c^+, S_p^+, S_r^+, L^+, I^+, T^+, R^+, I_s^+, I_p^+) \quad (22)$$

where

$$S_c^+ = \frac{k}{(d+\sigma_1+\sigma_2+\gamma_1)},$$

$$S_p^+ = \frac{\gamma_1k}{(\sigma_3+\sigma_4+d+\gamma_2)(d+\sigma_1+\sigma_2+\gamma_1)},$$

$$S_r^+ = \frac{\gamma_1\gamma_2k}{(d+\psi)(\sigma_3+\sigma_4+d+\gamma_2)(d+\sigma_1+\sigma_2+\gamma_1)},$$

$$L^+ = \frac{k(\sigma_1+\sigma_2)(\sigma_3+\sigma_4+d+\gamma_2)}{(d+\alpha)(\sigma_3+\sigma_4+d+\gamma_2)(d+\sigma_1+\sigma_2+\gamma_1)},$$

$$I^+ = \frac{k\alpha(\sigma_1+\sigma_2)(\sigma_3+\sigma_4+d+\gamma_2)}{(d+\alpha)(\sigma_3+\sigma_4+d+\gamma_2)(d+\sigma_1+\sigma_2+\gamma_1)(\theta_1+\omega+d+\delta+n)},$$

$$T^+ = \frac{k\alpha\theta_1(\sigma_1+\sigma_2)(\sigma_3+\sigma_4+d+\gamma_2)}{(d+\theta_2)(d+\alpha)(\sigma_3+\sigma_4+d+\gamma_2)(d+\sigma_1+\sigma_2+\gamma_1)(\theta_1+\omega+d+\delta+n)},$$

$$R^+ = \frac{A}{B},$$

where

$$A = k[\gamma_1\gamma_2\psi(d + \theta_1)(\sigma_1 + \sigma_2 + \gamma_1 + d)(\sigma_3 + \sigma_4 + d + \gamma_1)(\theta_1 + \omega + d + \delta + n) + \theta_1\theta_2(d + \gamma_1)(d + \gamma_2)(\psi + d)(\sigma_1 + \sigma_2)(\sigma_3 + \sigma_4 + d + \gamma_2)],$$

$$B = d(d + \gamma_2)(d + \gamma_1)(\psi + d)(d + \theta_1)(\alpha + d)(\sigma_1 + \sigma_2 + d + \gamma_1 + d)(\sigma_3 + \sigma_4 + \gamma_2 + d)(\theta_1 + \omega + d + \delta + n),$$

$$I_s^+ = \frac{nk\alpha(\sigma_1 + \sigma_2)(\sigma_3 + \sigma_4 + \gamma_2 + d)}{(\alpha + d)(\sigma_1 + \sigma_2 + \gamma_1 + d)(\sigma_3 + \sigma_4 + \gamma_2 + d)(\theta_1 + \omega + d + \delta + n)},$$

$$I_p^+ = \frac{\omega k\alpha(\sigma_1 + \sigma_2)(\sigma_3 + \sigma_4 + \gamma_2 + d)}{(\alpha + d)(\sigma_1 + \sigma_2 + \gamma_1 + d)(\sigma_3 + \sigma_4 + \gamma_2 + d)(\theta_1 + \omega + d + \delta + n)}.$$

3.5 Local stability of disease free equilibrium

The basic reproduction number influences the local stability of the disease-free equilibrium. The overall number of illnesses caused by one freshly contaminated pods brought into a healthy community is known as the basic reproduction number (\mathfrak{R}_o). Computation of \mathfrak{R}_o is carried out using the next generation matrix as laid out in [21-23]. \mathfrak{R}_o is obtained using

$$\mathfrak{R}_o = \rho(FV^{-1}) \quad (23)$$

where ρ is the spectral radius of the matrix FV^{-1} . Differential equations associated with L, I, T, I_s & I_p compartment are the infective classes and will be used in the computation of \mathfrak{R}_o .

$$\frac{dL}{dt} = \left(\frac{\beta_1 I_s}{P + I_s} + \frac{\beta_2 I_p}{P + I_p} \right) S_c + \left(\frac{\beta_3 I_s}{P + I_s} + \frac{\beta_4 I_p}{P + I_p} \right) S_p - (d + \alpha)L$$

$$\frac{dI}{dt} = \alpha L - (\theta_1 + \omega + d + \delta + n)I$$

$$\frac{dT}{dt} = \theta_1 I - (\theta_2 + d)T$$

$$\frac{dI_s}{dt} = nI - dI_s$$

$$\frac{dI_p}{dt} = \omega I - dI_p \quad (24)$$

Operator F_i is the rate at which new infection arises and V_i is the rate which compartments corresponding to the infection are exited with respect to (24).

$$F_i = \begin{pmatrix} \left(\frac{\beta_1 I_s}{P+I_s} + \frac{\beta_2 I_p}{P+I_p} \right) S_c + \left(\frac{\beta_3 I_s}{P+I_s} + \frac{\beta_4 I_p}{P+I_p} \right) S_p \\ 0 \\ 0 \\ 0 \\ 0 \end{pmatrix}, V_i = \begin{pmatrix} (d+\alpha)L \\ (\theta_1 + \omega + d + \delta + n)I - \alpha L \\ (\theta_2 + d)T - \theta_1 I \\ dI_s - nI \\ dI_p - \omega I \end{pmatrix}$$

Obtaining the partial derivative of F_i and V_i with respect to L, I, T, I_s, I_p , and later substituting the value of S_c, S_p, I_s and I_p at DFE, we obtain F and V as

$$F = \begin{pmatrix} 0 & 0 & 0 & \frac{\beta_1 k}{P(d+\gamma_1)} + \frac{\beta_3 \gamma_1 k}{P(d+\gamma_1)(d+\gamma_2)} & \frac{\beta_2 k}{P(d+\gamma_1)} + \frac{\beta_4 \gamma_1 k}{P(d+\gamma_1)(d+\gamma_2)} \\ 0 & 0 & 0 & 0 & 0 \\ 0 & 0 & 0 & 0 & 0 \\ 0 & 0 & 0 & 0 & 0 \\ 0 & 0 & 0 & 0 & 0 \end{pmatrix}$$

$$V = \begin{pmatrix} (\alpha+d) & 0 & 0 & 0 & 0 \\ -\alpha & (\theta_1 + \omega + d + \delta + n) & 0 & 0 & 0 \\ 0 & -\theta_1 & (\theta_2 + d) & 0 & 0 \\ 0 & -n & 0 & d & 0 \\ 0 & -\omega & 0 & 0 & d \end{pmatrix}$$

\mathfrak{R}_o , which is the dominant eigenvalue of equation (23), which is expressed as

$$\mathfrak{R}_o = \frac{k\alpha \left((P\beta_4\gamma_1 + \beta_2(d+\gamma_2))\omega + n(P\beta_3\gamma_1 + \beta_1(d+\gamma_2)) \right)}{Pd(\alpha+d)(\theta_1 + \omega + d + \delta + n)(d+\gamma_2)(d+\gamma_1)} \quad (25)$$

Remark 3.1 (i) if $\mathfrak{R}_o < 1$, the occurrence of infection on the pods will be decreasing,

(ii) If $\mathfrak{R}_o = 0$, the disease occurrence on the cocoa pod will be constant,

(iii) If $\mathfrak{R}_o > 1$, The infection on the pods will appear more frequently and last longer.

Theorem 3.3 The system's disease-free equilibrium in (5) is locally asymptotically stable if and only if $\mathfrak{R}_o < 1$ and

unstable when $\mathfrak{R}_o > 1$.

See [21, 24-25] for details on proving of theorem 3.3.

3.6 Global stability analysis

The Lyapunov function already utilized for other models [21, 24-25] is adopted to prove the global asymptotically stability of model (5) for both Disease free and Endemic equilibrium point.

Theorem 3.4 Disease free equilibrium points of ststem (5) is globally asymptotically stable in Ω whenever $\mathfrak{R}_o \leq 1$.

Proof. Using the Lyapunov candidate

$$\begin{aligned}
 V &= \frac{1}{2} \left[(S_c - S_c^o) + (S_p - S_p^o) + (S_r - S_r^o) + (L - L^o) + (I - I^o) + (T - T^o) + (R - R^o) + (I_s - I_s^o) + (I_p - I_p^o) \right]^2 \\
 \frac{dV}{dt} &= \left[(S_c - \frac{k}{d + \gamma_1}) + (S_p - \frac{\gamma_1 k}{(d + \gamma_1)(d + \gamma_2)}) + (S_r - \frac{\gamma_2 \gamma_1 k}{(d + \gamma_1)(d + \gamma_2)(d + \psi)}) + L + I + T + (R - R^o) \right. \\
 &\quad \left. + (I_s - I_s^o) + (I_p - I_p^o) \right] \frac{dN}{dt} \\
 &= \left[(S_c - S_c^o) + (S_p - S_p^o) + (S_r - S_r^o) + (L - L^o) + (I - I^o) + (T - T^o) + (R - R^o) + (I_s - I_s^o) + (I_p - I_p^o) \right] \frac{dN}{dt} \\
 &= \left[(S_c - \frac{k}{d + \gamma_1}) + (S_p - \frac{\gamma_1 k}{(d + \gamma_1)(d + \gamma_2)}) \right. \\
 &\quad \left. + (S_r - \frac{\gamma_2 \gamma_1 k}{(d + \gamma_1)(d + \gamma_2)(d + \psi)}) + L + I + T + (R - \frac{\psi \gamma_2 \gamma_1 k}{d(d + \gamma_1)(d + \gamma_2)(d + \psi)}) + I_s + I_p \right] \frac{dN}{dt}
 \end{aligned}$$

After simplification, we have

$$\begin{aligned}
 \frac{dV}{dt} &\leq \left[N - \frac{k}{d} \right] [k - dN] \\
 &\leq -\frac{1}{d} (k - dN)^2
 \end{aligned} \tag{26}$$

Therefore

$$V \leq 0$$

Hence, $V \leq 0$, if k, d, N are positive, this implies that the function V is strictly Lyapunov function which indicates the disease free equilibrium point (E^o) is globally asymptotically stable. \square

Theorem 3.5 Whenever $\mathfrak{R}_o > 1$, the Endemic equilibrium point is globally asymptotically stable in Ω .

Proof. Considering the Lyapunov candidate

$$\begin{aligned}
V = & (S_c - S_c^+ \ln S_c) + (S_p - S_p^+ \ln S_p) + (S_r - S_r^+ \ln S_r) + p_1(L - L^+ \ln L) + p_2(I - I^+ \ln I) + p_3(T - T^+ \ln T) \\
& + p_4(R - R^+ \ln R) + p_5(I_s - I_s^+ \ln I_s) + p_6(I_p - I_p^+ \ln I_p)
\end{aligned} \tag{27}$$

defined and continuous for all $S_c, S_p, S_r, L, I, T, R, I_s, I_p > 0$ and satisfies

$$\frac{dV}{dt} = \frac{\partial V}{\partial S_c} \frac{dS_c}{dt} + \frac{\partial V}{\partial S_p} \frac{dS_p}{dt} + \frac{\partial V}{\partial S_r} \frac{dS_r}{dt} + \frac{\partial V}{\partial L} \frac{dL}{dt} + \frac{\partial V}{\partial I} \frac{dI}{dt} + \frac{\partial V}{\partial T} \frac{dT}{dt} + \frac{\partial V}{\partial R} \frac{dR}{dt} + \frac{\partial V}{\partial I_s} \frac{dI_s}{dt} + \frac{\partial V}{\partial I_p} \frac{dI_p}{dt} \tag{28}$$

thus,

$$\begin{aligned}
\frac{dV}{dt} = & \left(1 - \frac{S_c^+}{S_c}\right) \frac{dS_c}{dt} + \left(1 - \frac{S_p^+}{S_p}\right) \frac{dS_p}{dt} + \left(1 - \frac{S_r^+}{S_r}\right) \frac{dS_r}{dt} + p_1 \left(1 - \frac{L^+}{L}\right) \frac{dL}{dt} + p_2 \left(1 - \frac{I^+}{I}\right) \frac{dI}{dt} + \\
& p_3 \left(1 - \frac{T^+}{T}\right) \frac{dT}{dt} + p_4 \left(1 - \frac{R^+}{R}\right) \frac{dR}{dt} + p_5 \left(1 - \frac{I_s^+}{I_s}\right) \frac{dI_s}{dt} + p_6 \left(1 - \frac{I_p^+}{I_p}\right) \frac{dI_p}{dt} \\
= & \left(1 - \frac{S_c^+}{S_c}\right) [k - (d + \sigma_1 + \sigma_2 + \gamma_1)S_c] + \left(1 - \frac{S_p^+}{S_p}\right) [\gamma_1 S_c - (\sigma_3 + \sigma_4 + \gamma_2 + d)S_p] + \\
& \left(1 - \frac{S_r^+}{S_r}\right) [\gamma_2 S_p - (d + \psi)S_r] + p_1 \left(1 - \frac{L^+}{L}\right) [(\sigma_1 + \sigma_2)S_c + (\sigma_3 + \sigma_4)S_p - (\alpha + d)L] + \\
& p_2 \left(1 - \frac{I^+}{I}\right) [\alpha L - (n + \omega + \theta_1 + d + \delta)I] + p_3 \left(1 - \frac{T^+}{T}\right) [\theta_1 I - (\theta_2 + d)T] + \\
& p_4 \left(1 - \frac{R^+}{R}\right) [\psi S_r + \theta_2 T - dR] + p_5 \left(1 - \frac{I_s^+}{I_s}\right) [nI - dI_s] + p_6 \left(1 - \frac{I_p^+}{I_p}\right) [\omega I - dI_p]
\end{aligned} \tag{29}$$

At endemic equilibrium

$$k - (d + \sigma_1 + \sigma_2 + \gamma_1)S_c = 0$$

therefore

$$k = (d + \sigma_1 + \sigma_2 + \gamma_1)S_c \tag{30}$$

Substituting equation (29) into equation (28) and simplifying yields

$$\begin{aligned} \frac{dV}{dt} \leq & -\left[1 - \frac{S_c^+}{S_c}\right](S_c - S_c^+)(d + \sigma_1 + \sigma_2 + \gamma_1) + \left(\frac{S_p^+}{S_p} - 1\right)\gamma_1 S_c + (S_p - S_p^+)(d + \sigma_3 + \sigma_4 + \gamma_2) \\ & \left(\frac{S_r^+}{S_r} - 1\right)\gamma_2 S_p + (S_r - S_r^+)(d + \psi) + p_1\left(1 - \frac{L^+}{L}\right)(\sigma_1 + \sigma_2)S_c + p_1\left(1 - \frac{L^+}{L}\right)(\sigma_3 + \sigma_4)S_p + p_1(L - L^+)(\alpha + d) \\ & + p_2\left(1 - \frac{I^+}{I}\right)\alpha L + p_2(I - I^+)(\theta_1 + \omega + d + \delta + n) + \left(\frac{T^+}{T} - 1\right)\theta_1 I + p_3(T - T^+)(d + \theta_2) \\ & p_4\left(\frac{R^+}{R} - 1\right)\psi S_r + p_4\left(\frac{R^+}{R} - 1\right)\theta_2 + p_4(R - R^+)d + p_5\left(\frac{I_s^+}{I_s} - 1\right)nI + p_6(I_p - I_p^+)d \\ & + p_6\left(\frac{I_p^+}{I_p} - 1\right)\omega I + p_5(I_s - I_s^+)d \end{aligned}$$

therefore,

$$\frac{dV}{dt} \leq 0$$

Hence, $V < 0$ for $p_1, p_2, p_3, p_4, p_5, p_6 > 0$. Note that, $V = 0$ if and only if $S_c = S_c^+, S_p = S_p^+, S_r = S_r^+, L = L^+, I = I^+, T = T^+, R = R^+, I_s = I_s^+$, and $I_p = I_p^+$. Therefore the largest compact invariant set in $(S_c, S_r, S_p, L, I, T, R, I_s, I_p) \in \Omega : V = 0$ is the singleton E^+ , where E^+ is the endemic equilibrium, by LaSalle's invariant principle this signifies that E^+ is globally asymptotically stable in the interior of Ω . \square

4. Sensitivity analysis

\mathfrak{R}_o is the epidemic threshold that the controls spread, understanding various disease transmissions, and the variables help determine the most effective control approach. Predicting the sensitivities of each component involved in \mathfrak{R}_o is crucial. Sensitivity analysis measures how much a variable has changed to how much the factors have changed.

Definition 4.1 The following formula is used to explain the standardized forward sensitivity index of a variable B that is dependent on a parameter m in different ways: [20, 26].

$$Z_m^B = \frac{\partial B}{\partial m} \times \frac{m}{B} \quad (31)$$

The sensitivity indices of reproduction number \mathfrak{R}_o corresponding to our model parameters is given as

$$Z_k^{\mathfrak{R}_o} = \frac{\partial \mathfrak{R}_o}{\partial k} \times \frac{k}{\mathfrak{R}_o} = +1.0000 \quad (32)$$

In a similar approach, we obtain the remaining indices for the model parameters as displayed in Table 1.

The value of \mathfrak{R}_o increases when the index with a positive indication are increased, also the value of \mathfrak{R}_o reduces

when the index with a negative indication are increased, thus making the parameters with negative indices a importance parameter used in the control of the disease.

The most sensitive parameters of our model are P , α , γ_1 , γ_2 , d , θ_1 , n , ω and δ , since it is not practical to increase most of the parameters, thus reducing \mathfrak{R}_o is a function of θ_1 and δ . The result suggested that intervention strategy should be targeted at treating infected pods with fungicide and infected pod removal.

Table 1. Sensitivity indices of \mathfrak{R}_o

Parameters	Sensitivity indices
k	+1.0000
d_o	-1.7734
ω	+0.0333
δ	-0.0101
ψ	-0.0452
β_1	+0.5433
β_2	+0.4742
β_3	+0.0034
β_4	+0.0015
θ_1	-0.0115
γ_1	-0.1743
γ_2	0.000
γ_3	-0.0312
P	-1.0000

5. Numerical simulation

In this part, we use numerical simulation to examine the effect of several variables on the dispersal of the black pod infection. The following starting points are used in these experiments:

$$S_c(0) = 100, S_p(0) = 0, S_r(0) = 0, L(0) = 0, I(0) = 0, T(0) = 0, R(0) = 0, I_s(0) = 20, I_p(0) = 0$$

and the baseline parameter value are taken from Table 2. Computation were run in Mat-lab with the ODE45 routine, this function implement a Runge-kutta method with a variable time step for efficient computation.

Table 2. Description of parameters

parameter	Unit	value/range of value	Source
k	Day ⁻¹	12	[27]
d	Day ⁻¹	0.05	[28]
β_1	Day ⁻¹	0.05	[8]
β_2	Day ⁻¹	0.05	[8]
β_3	Day ⁻¹	0.02	[8]
β_4	Day ⁻¹	0.02	[8]
γ_1	Day ⁻¹	0.05	[28-29]
γ_2	Day ⁻¹	0.027	[28]
ψ	Day ⁻¹	0.01	Assumed
θ_1	Day ⁻¹	0.1	Assumed
θ_2	Day ⁻¹	0.09	Assumed
n	SporesDay ⁻¹	0.4	[8]
ω	SporesDay ⁻¹	0.4	[8]
δ	Day ⁻¹	[0-0.8]	[8]
P	No. of Spores	[0 – 10 ¹⁰]	[8]
α	Day ⁻¹	0.05	Assumed

Figure 2 demonstrates that the number of infected pods decreases with increasing δ values.

According to Figure 3, treating infected pods more quickly causes a reduction in the number of infected pods within the first 40 days. The first 40 days after $\theta_1 = 0$ saw the maximum number of infected pods. Thus, treating diseased pods regularly (by applying fungicide) can stop the infection from spreading. It is advised to treat infected pods as soon as possible because doing so will lessen the infection's threat.

In Figure 4, it can be seen that changing the value of θ_1 has a noticeable impact on the removed compartment in the first 180 days. It can also be inferred from the plot that the higher the value of θ_1 , the sooner the pods will be ready for harvest, meaning that they will grow more quickly and reach maturity on schedule.

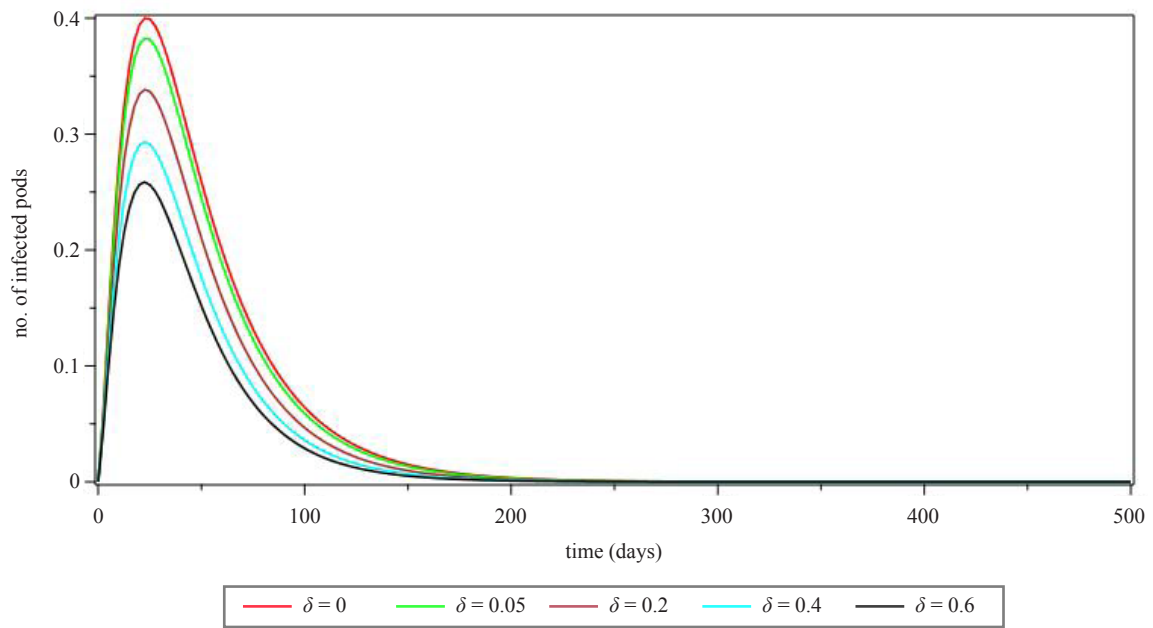


Figure 2. Solution plot of $I(t)$ in model (5) showing effect of δ

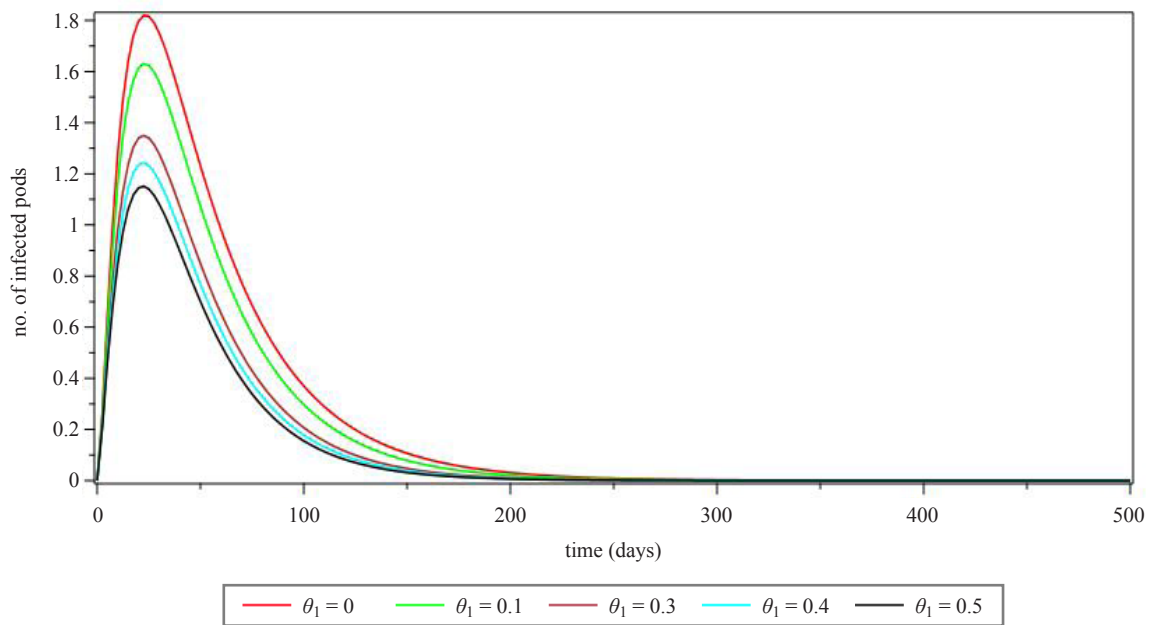


Figure 3. Solution plot of $I(t)$ in model (5) showing effect of θ_1

Figure 5 shows that different ψ values have a noticeable impact on the removed compartment. As a result, consistent and routine harvesting of healthy, ripe pods is necessary to lower the number of infected.

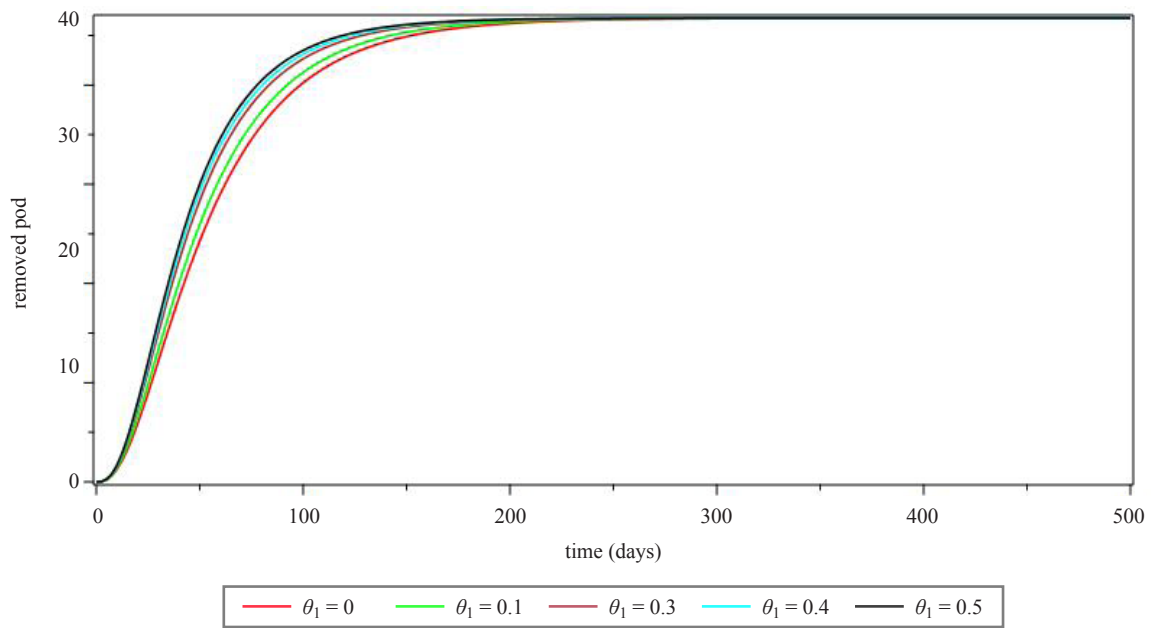


Figure 4. Solution plot of $R(t)$ in model (5) showing effect of θ_1

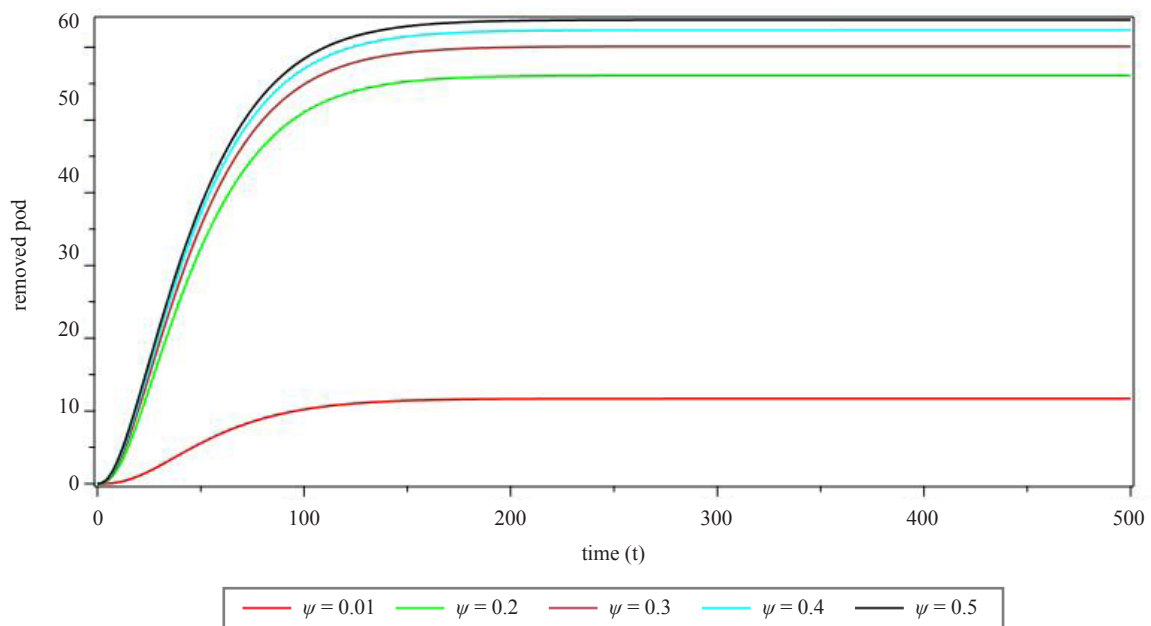


Figure 5. Solution plot of $R(t)$ in model (5) showing effect of ψ_1

6. Findings of study

The study's findings are as follows:

- (i) effort at controlling the spread of the disease should be focus on fungicide application
- (ii) in all cases where the basic reproduction number is less than 1, the black pod free equilibrium is asymptotically

stable.

(iii) regular harvest of healthy pod is a necessity and one of the efficient approach to control the menace of the disease.

(iv) the spread of the disease is positively correlated to $k, \beta_1, \beta_2, \beta_3, \beta_4, n, \omega$ it is negatively correlated to $P, \alpha, \gamma_1, \gamma_2, d, \theta_1, n, \omega$ and δ .

7. Discussion of results

In order to explore the dynamics of black pod disease among cocoa pods, a nonlinear mathematical model has been developed in this research. It is noted that whenever the basic reproduction number is less than one, the model has a unique disease-free equilibrium point that is locally asymptotically stable. It is also observed that the most influential factor on the spread of the disease are natural pod death rate d , Michaelis constant for fungi infection transmission P , rate of transmission from latent pod to infected pod α , transmission rate from cherelles state to young and mature pod γ_1 , transmission from young and mature pods to ripe pods γ_2 , rate at which the infected is treated θ_1 , releasing rate of spore shedding n , speed rate of spore shedding ω and pod removal rate δ .

8. Conclusion

To sum up, mathematical modeling is a useful tool for comprehending the dynamics of cocoa black pod disease transmission. Researchers and farmers can more accurately estimate how the disease will affect cocoa yields by using mathematical models to better understand how the disease spreads. This can aid in the creation of efficient disease management techniques, such as pinpointing the right moment to apply fungicides and choosing the ideal sites for the implantation of new cocoa trees. The impact of environmental elements on the disease, such as wind, temperature, and rainfall, can also be studied using mathematical models. This can assist predict disease outbreaks and lessen their effects. Overall, mathematical modeling is a crucial tool for controlling cocoa black pod disease and making sure that cocoa output is sustainable.

Future research should focus on incorporating spatial factors into the equation. Considering geographical variations, landscape features, and proximity to other cocoa plantations will provide a more realistic representation of the disease's spread. Spa-tial models can aid in predicting potential disease outbreaks and optimizing control measures across different cocoa-growing regions.

Acknowledgments

Numerous stakeholders have contributed to and supported this research in an effort to improve the findings. We appreciate all the help and encouragement you have given.

Conflict of interest

The authors declare no competing financial interest.

References

- [1] Essama-Nssah B, Gockowski J, Kelly LA. *A New Deal for Cameroons Forests, Managing a Global Resource*. Routledge; 2019.
- [2] Frost S, Nyadanu D. Cocoa black pod disease: A review of epidemiology, symptomatology, and management of

Phytophthora palmivora. *Plants*. 2019; 8(4): 98-125.

- [3] Adu-Acheampong R, Galyuon IK, Dadzie AM. Cocoa black pod disease: Challenges and opportunities towards sustainable management in West Africa. *Plant Pathology*. 2019; 68(5): 805-815.
- [4] Phillips-Mora W, Wilkinson MJ. Frosty pod of cacao: A disease with a limited geographic range but unlimited potential for damage. *American Phytopathological Society*. 2019; 97(12): 1644-1751. Available from: doi:10.1094/PHYTO-97-12-1644.
- [5] Pokou DN, Fister AS, Winters N, Tahi M, Klotioloma C, Sebastian A, et al. Resistant and susceptible cacao genotypes exhibit defense gene polymorphism and unique early responses to Phytophthora megakarya inoculation. *Plant Molecular Biology*. 2019; 99: 499-516.
- [6] Afoakwa EO. *Cocoa Production and Processing Technology*. 1st ed. CRC Press, Taylor & Francis Group, USA; 2014.
- [7] Kozicka M, Tacconi F, Horna D, Gotor E, Klotioloma C, Sebastian A, et al. *Forecasting Cocoa Yields for 2050*. Bioversity International, Rome, Italy; 2018.
- [8] Nembot C, Takam Soh P, Ten Hoopen GM, Dumont G. Modeling the temporal evolution of Cocoa black pod rot disease caused by Phytophthora Magakarya. *Mathematical Methods in the Applied Sciences*. 2018; 41(18): 8818-8843.
- [9] Kermack WO, McKendrick AG. A contribution to the mathematical theory of epidemics. *Proceedings of the Royal Society of London. Series A, Containing Papers of a Mathematical and Physical Character*. 1927; 115(772): 700-721. Available from: doi:10.1098/rspa.1927.0118.
- [10] Etaware PM, Adedeji AR, Osowole OI. ETAPOD: A forecast model for prediction of black pod disease outbreak in Nigeria. *PLoS ONE*. 2020; 15(1): e020-e024. Available from: doi:10.1371/journal.pone.0209306.
- [11] Mahendran SA, Payne RW, Maree HJ. Modeling the spread of cocoa black pod disease using Bayesian networks. *Phytopathology*. 2018; 108(11): 1314-1324.
- [12] Matofali AX. Modelling and optimal control of insect transmitted plant disease. *Open Science Journal of Mathematics and Application*. 2020; 8(1): 1-9.
- [13] Nakazawa T, Urano S, Yamanaka T. *Model Analysis for Plant Disease Dynamics Co-Mediated by Herbivory and Herbivore-Borne Phytopathogens*. Biodiversity Division, National Institute for Agro Environmental sciences, Kannondai, Tsukuba, Japan; 2012.
- [14] Meng X, Zhong T, Song Y, li Z. The dynamics of plant disease models with continuous and Impulsive cultural control strategies. *Journal of Theoretical Biology*. 2010; 266(1): 29-40. Available from: doi:10.1016/j.jtbi.2010.05.033.
- [15] Oduro B, Apenteng OO, Nkansah H. Assessing the effect of fungicide treatment on Cocoa black pod disease in Ghana. *Statistics, Optimization and Information Computing*. 2020; 8(2): 374-385. Available from: doi:10.19139/soic-2310-5070-686.
- [16] Hethcote HW. The mathematics of infectious diseases. *SIAM Review*. 2000; 42(4): 599-653. Available from: doi:10.1137/S0036144500371907.
- [17] Ibrahim OM, Okuonghae D, Ikhile M. Mathematical modeling of the population dynamics of age-structured criminal gangs with correctional intervention. *Applied Mathematical Modeling*. 2022; 107: 39-71. Available from: doi:10.1016/j.apm.2022.02.005.
- [18] Kalu AU, Agwu IA, Agbanyim AN. Mathematical analysis of the endemic equilibrium of the transmission dynamics of tuberculosis. *International Journal of Scientific and Technology Research*. 2013; 2: 263-269.
- [19] Daley DJ, Gani J. *Epidemic Modeling-An Introduction*. Cambridge University Press, Cambridge; 2005.
- [20] Adedeji-Adenola H, Olugbake OA, Adeosun SA. Factors influencing COVID-19 vaccine uptake among adults in Nigeria. *PLoS ONE*. 2022; 17(2): 26-43.
- [21] Akingbade JA, Ogundare BS. Boundedness and stability properties of solutions of mathematical model of measles. *Tamkang Journal of Mathematics*. 2021; 51(1): 91-112.
- [22] Van den Driessche P, Watmough J. Reproduction numbers and sub-threshold endemic equilibria for compartmental models of disease transmission. *Mathematical Biosciences*. 2002; 180(1-2): 29-48. Available from: doi:10.1016/S0025-5564(02)00108-6.
- [23] Heesterbeek JA, Dietz K. The concept of R_0 in epidemic theory. *Statistica Neerlandica*. 1996; 50(1): 89-110. Available from: doi:10.1111/j.1467-9574.1996.tb01482.x.
- [24] Kashif butt AI, Batool S, Imran M, Al Nuwairan M. Design and analysis of a new COVID-19 model with comparative study of control Strategies. *Mathematics*. 2023; 11(1978): 1-29.
- [25] Kashif butt AI, Aftab H, Imran M, Ismaeel T. Mathematical study of lumpy skin disease with optimal control

- analysis through vaccination. *Alexandria Engineering Journal*. 2023; 72: 247-259.
- [26] Chitnis N, Hyman JM, Cushing JM. Determining important parameters in the spread of malaria through the sensitivity analysis of a mathematical model. *Bulletin of Mathematical Biology*. 2000; 70: 1272-1296. Available from: doi:10.1007/s11538-008-9299-0.
- [27] Bisselua D, Yede D, Vidal S. Dispersion models and sampling of cacao mirid bug *Sahlbergella singularis* (hemiptera: Miridae) on theobroma cacao in southern cameroon. *Environmental Entomology*. 2011; 10: 111-119.
- [28] Takam Soh E, Ndong Nguema P, Gwet H, Ndoumbe-Nkeng H. Smooth estimation of a lifetime distribution with competing risks by using regular interval observations: Application to cocoa fruits growth. *Journal of the Royal Statistical Society Series C*. 2013; 62(5): 741-760. Available from: doi:10.1111/rssc.12019.
- [29] Ten Hoopen G, Deberdt P, Mbenoum P, Cilas C. Modelling cacao pod growth: Implications for disease control. *Annals of Applied Biology*. 2012; 160(3): 260-272. Available from: doi:10.1111/j.1744-7348.2012.00539.x.